
A delayed remap technique in multi-material ALE methods

Ahlem Alia* — Nicolas Aquelet** — Mhamed Souli*
Lars Olovsson**

* *Laboratoire de Mécanique de Lille UMR CNRS 8107
Boulevard Paul Langevin, Cité Scientifique
F-59655 Villeneuve d'Ascq cedex
ahlem.alia@ed.univ-lille1.fr, mahmed.souli@univ-lille1.fr*

***Livermore Software Technology Corporation
7374 Las Positas Road, Livermore, CA 94550, USA
aquelet@lstc.com, lars@lstc.com*

ABSTRACT. A new mesh refinement method for multi-material ALE formulations is presented. The computational timestep of this approach is divided in 2 steps: a so-called Lagrangian step, during which the mesh deforms with the update of the solution, and a so-called Eulerian step, during which the mesh is remapped in order to preserve the mesh regularity and refine in the vicinity of the shock front. As test case the method is applied to the propagation of an explosive airblast, for which experimental results are available.

RÉSUMÉ. L'article décrit une nouvelle méthode de raffinement de maillage pour des formulations ALE multimatérielles explicites. Le pas de calcul de cette approche est divisé en 2 temps : un pas dit Lagrangien au cours duquel le maillage se déforme avec la mise à jour de la solution, et un pas dit Eulérien au cours duquel le maillage est déplacé de manière à préserver la régularité du maillage et à le raffiner dans le voisinage du choc. Au cours de ce pas, la solution est projetée sur le nouveau maillage. Cette méthode est appliquée à la propagation d'une onde de choc explosive pour laquelle des résultats expérimentaux existent.

KEYWORDS: mutli-material ALE formulation, delayed mesh relaxation, shock capture, adapted mesh refinement.

MOTS-CLÉS : formulation ALE multimatérielle, relaxation retardée du maillage, capture du choc, raffinement adapté du maillage.

1. Introduction

The principle of an ALE¹ code is based on the independence of the Finite Element mesh movement with respect to the material motion. In fact, the freedom of moving the mesh offered by the ALE formulation enables a combination of advantages of Lagrangian and Eulerian methods.

In the Lagrangian description of motion the computational domain follows the material motion, which greatly simplifies the governing equations. Lagrangian schemes have proven very accurate as long as the mesh remains regular. However, the material may undergo large deformations that lead to severe mesh distortions and thereby accuracy losses and a reduction of the critical time step, which is the amount of time necessary for an acoustic wave to cross the smallest element in the mesh (the Courant Friedrichs Levy condition).

With an Eulerian description of motion the mesh is fixed in space and the material passes through the element grid. The transport of mass between elements complicates the governing equations by introducing nonlinear transport terms. Mass conservation is not automatically satisfied. Advection algorithms need to be implemented for the mass, momentum and internal energy conservation and for the tracking of all state variables.

According to (Wilkins, 1964), the accuracy of Eulerian codes are comparable to the accuracy of Lagrangian codes in hydrodynamic applications, when using higher order advection algorithms. Furthermore, since the reference system is fixed, the Eulerian formulation preserves the mesh regularity. The main drawbacks are the computational cost per cycle and the dissipation errors generated when treating the advective terms in the governing equations.

Eulerian and ALE hydrocodes split each computational timestep into two phases. The first step is the Lagrangian phase, where the material motion and the mesh motion are identical and where the incremental motion of the material is computed. All physical phenomena as well as boundary conditions are considered during this phase.

The second step is the Eulerian phase, which is referred to as the advection, or remap phase. In this step the mesh is moved independently to the material motion and there is a transport of material between the cells. This corresponds to the treatment of the convective terms introduced in the governing equations.

Pioneering work on the ALE formulation were presented by (Hughes, 1981; Liu, 1988) to solve free surface problems for incompressible viscous flow, by (Benson, 1992; Belytschko, 1982) to treat fluid-structure interaction problems. A detailed survey of ALE Finite Element methods was presented by (Donea, 1983). Hughes *et al.*, developed a streamlined upwind Petrov-Galerkin method (Brook, 1982; Mallet,

1. Arbitrary Lagrange Euler

1985; Hughes, 1986), which was implemented in an ALE formulation by (Liu, 1988). The formulation has been applied for several applications in automotive, aerospace and biomedical industries for free surface modeling, sloshing tanks, fluid-structure coupling applications and for high velocity impact and penetration problems. An explicit ALE formulation has been applied by (Souli *et al.*, 2000), for high velocity impacts of elasto-plastic materials and for the analysis of sloshing tanks in aerospace applications.

This paper presents a new mesh relaxation method for explicit multi-material Arbitrary Lagrangian-Eulerian (ALE) Finite Element simulations. The proposed method is valid for structured and unstructured meshes and it is designed with the objective to reduce numerical dissipation errors when analyzing the propagation of shock fronts. The method aims to delay the advection phase in the vicinity of shock fronts in order to obtain an as “Lagrange like” behavior as possible near the shock, while at the same time keeping the mesh distortions on an acceptable level.

The outline of this paper is as follows. In Section 2 an overview of the governing equations in the ALE description of motion are presented. Section 3 describes the technique of delaying the mesh relaxation. In Section 4 the numerical modeling of a high explosive detonation in air using a structured ALE cartesian grid is presented, illustrating the performance of the introduced relaxation technique. In this application the airblast loads a steel plate and a comparison with available experimental data (Boyd, 2000) was possible.

2. Multi-material ALE description of Navier-Stokes equations

2.1. ALE formulation

In the ALE description of motion, an arbitrary referential coordinate is introduced in addition to the Lagrangian and Eulerian coordinates (Hughes *et al.*, 1981; Souli, 2000). The total time derivative of a variable f with respect to a reference coordinate can be described as Equation [1]:

$$\frac{df(\vec{X},t)}{dt} = \frac{\partial f(\vec{x},t)}{\partial t} + (\vec{v} - \vec{w}) \cdot \overrightarrow{\text{grad}} f(\vec{x},t) \quad [1]$$

where \vec{X} is the Lagrangian coordinate, \vec{x} is the ALE coordinate, \vec{v} is the particle velocity and \vec{w} is the velocity of the reference coordinate, which will represent the grid velocity for the numerical simulation, and the system of reference will be later the ALE grid. Thus substituting the relationship between the total time derivative and the reference configuration time derivative derives the ALE equations.

Let $\Omega^f \in R^3$, represent the domain occupied by the fluid, and let $\partial\Omega^f$ denote its boundary. The equations of mass, momentum and energy conservation for a Newtonian fluid in ALE formulation in the reference domain, are given by:

$$\frac{\partial \rho}{\partial t} + \rho \operatorname{div}(\vec{v}) + (\vec{v} - \vec{w}) \operatorname{grad}(\rho) = 0 \quad [2]$$

$$\rho \frac{\partial \vec{v}}{\partial t} + \rho (\vec{v} - \vec{w}) \cdot \overline{\operatorname{grad}}(\vec{v}) = \overline{\operatorname{div}}(\overline{\overline{\sigma}}) + \vec{f} \quad [3]$$

$$\rho \frac{\partial e}{\partial t} + \rho (\vec{v} - \vec{w}) \cdot \overline{\operatorname{grad}}(e) = \overline{\overline{\sigma}} : \overline{\operatorname{grad}}(\vec{v}) + \vec{f} \cdot \vec{v} \quad [4]$$

where ρ is the density and $\overline{\overline{\sigma}}$ is the total Cauchy stress given by:

$$\overline{\overline{\sigma}} = -p \cdot Id + \mu \left(\overline{\operatorname{grad}}(\vec{v}) + \overline{\operatorname{grad}}(\vec{v})^T \right) \quad [5]$$

where p is the pressure and μ is the dynamic viscosity. Equations [2]-[4] are completed with appropriate boundary conditions. The part of the boundary at which the velocity is assumed to be specified is denoted by $\partial\Omega_1^f$. The inflow boundary condition is:

$$\vec{v} = \vec{g}(t) \quad \text{on} \quad \partial\Omega_1^f \quad [6]$$

The traction boundary condition associated with Equation [4] are the conditions on stress components. These conditions are assumed to be imposed on the remaining part of the boundary.

$$\overline{\overline{\sigma}} \cdot \vec{n} = \vec{h}(t) \quad \text{on} \quad \partial\Omega_2^f \quad [7]$$

One of the major difficulties in time integration of the ALE Navier-Stokes equations [2]-[4] is due to the nonlinear term related to the relative velocity $(\vec{v} - \vec{w})$. For some ALE formulations, the mesh velocity can be solved using a remeshing and smoothing process. In the Eulerian formulation, the mesh velocity $\vec{w} = \vec{0}$, this assumption eliminates the remeshing and smoothing process, but does not simplify the Navier-Stokes equations [2]-[4]. To solve equations [2]-[4], the split approach detailed in (Benson, 1992; Hughes, 1981) and implemented in most hydrocodes such as LS-DYNA® is adopted in this paper. Operator splitting is a convenient method for breaking complicated problems into series of less complicated problems. In this approach, first a Lagrangian phase is performed, using an explicit finite element

method, in which the mesh moves with the fluid particle. In the CFD community, this phase is referred to as a linear Stokes problem. In this phase, the changes in velocity, pressure and internal energy due to external and internal forces are computed. The equilibrium equations for the Lagrangian phase are:

$$\rho \frac{d\vec{v}}{dt} = \overline{\text{div}(\vec{\sigma})} + \vec{f} \tag{8}$$

$$\rho \frac{de}{dt} = \overline{\vec{\sigma} : \text{grad}(\vec{v})} + \vec{f} \cdot \vec{v} \tag{9}$$

The mass conservation equation is used in its integrated form Equation [11] rather than as a partial differential equation (Belytschko *et al.*, 2001). Although the continuity equation can be used to obtain the density in a Lagrangian formulation, it is simpler and more accurate to use the integrated form Equation [10] in order to compute the current density ρ :

$$\rho J = \rho_0 \tag{10}$$

where ρ_0 is the initial density and J is the volumetric strain given by the Jacobian:

$$J = \det \left(\frac{\partial x_i}{\partial X_j} \right) \tag{11}$$

In the second phase, called advection or transport phase, the transportation of mass, momentum and energy across element boundaries are computed. This may be thought of as remapping the displaced mesh at the Lagrangian phase back to its initial position. The transport equations for the advection phase are:

$$\begin{aligned} \frac{\partial \phi}{\partial t} + \vec{c} \cdot \overline{\text{grad}}(\phi) &= 0 \\ \phi(\vec{x}, 0) &= \phi_0(x) \end{aligned} \tag{12}$$

where $\vec{c} = \vec{v} - \vec{w}$ is the difference between the fluid velocity \vec{v} , and the velocity of the computational domain \vec{w} , which will represent the mesh velocity in the finite element formulation. In some papers (Hughes *et al.*, 1981; Belytschko *et al.*, 2001) \vec{c} is referred as the convective velocity. The hyperbolic equation system [12] is solved by using a finite volume method. Either a first order upwind method or second order Van Leer advection algorithm (Van Leer, 1977) can be used to solve Equation [12]. The advection method is successively applied for the conservative variables: mass, momentum and energy with initial condition $\phi_0(x)$, which is the

solution from the Lagrangian calculation of equations [8]-[9] at the current time. In Equation [12], the time t is a fictitious time: in this paper, time step is not updated when solving for the transport equation. There are different ways of splitting the Navier-Stokes problems. In some split methods, each of the Stokes problem and transport equation are solved successively for half time step.

2.2. Multi-material ALE formulation

Problems, in which interfaces between different materials are present, are more easily modelled by using a Lagrangian method. However if the analysis involves large material deformation, the distortion of the Lagrangian mesh makes such a method difficult to use. Many re-meshing steps could be necessary for the Lagrangian calculation to continue. Another method to use is the multi-material ALE formulation. The relaxation technique presented in this work is mainly designed for this formulation. The multi-material formulation is a method that allows more than one material in each cell. It is powerful by the fact that complex geometries can be described without an element grid matching the material interface. The multi-material concept is used in many hydrocodes, but its implementation is more complex than a single material formulation. Also the memory requirement is higher, since each cell must be prepared to store more than one set of state variables. The multi-material method involves dealing with two new issues: the interface tracking and the advection of fluid materials across element boundaries.

There are several methods to treat the free surface in a fluid problem; the common one is the VOF (Volume Of Fraction) method, which is attractive for solving a broad range of non-linear problems in fluid and solid mechanics, because it allows arbitrary large deformations and enables free surfaces to evolve. The Lagrangian phase of the VOF method is easily implemented in an explicit ALE finite element method. Before advection, special treatment for the partially voided element is needed. An element containing a material interface is partially filled and the volume fraction satisfies $V_f \leq 1$. In order to compute accurately the position of the material interface, interface-tracking algorithm is performed before the remesh process and advection phase. A possible way of tracking interfaces is the use of the volume fractions of the elements, or the Young method (Young, 1982). In this method, the material layout is described solely by the volume fraction of the fluid material in the element. Specifically, a plane approximates the interface in the cell. Then nodal volume fractions are computed to each node based on the fraction volumes of elements that share the same node. The nodal volume fractions determine the slope of the material interface inside the element. The position of the interface is then adjusted so that it divides the element into two volumes, which correctly matches the element volume fraction.

The interface position is used to calculate the volume of the fluid flowing across cell sides. As the X-advection, Y-advection and Z-advection are calculated in

separate steps, it is sufficient to consider the flow across one side only by taking the interface position into account. The fluxes of conservative variables for each material are computed by evaluating the volumes given by the intersection of the material interface and the total volume of the flux transported to the adjacent element.

3. Fluid – porous structure interaction

The ALE relaxation technique presented in this section is a general method for structured and unstructured meshes in one-, two- and three-dimensional contexts. The method has been implemented and tested in the explicit Finite Element code LS-DYNA®, which uses the second order accurate central difference scheme for the time integration. To fully enjoy the benefits of an explicit time integration scheme, the mass is assumed concentrated at the nodes. This leads to a diagonal mass matrix, which greatly simplifies the relation between nodal forces and accelerations.

3.1. Lagrangian phase

In the Lagrangian phase of a cycle, the solution is advanced from t^n to t^{n+1} , without any iterations and without solving any global equation systems. For numerical stability reasons, the magnitude of the time step, Δt^{n+1} , is limited by the highest eigenfrequency of the system or by flux limits in the advection algorithm. To save memory, a staggered scheme in time is used. Velocities are computed at $t^{n+1/2}$ and accelerations and coordinates at t^{n+1} . Knowing the mass m^n of the node and the force \vec{f}^n acting on it, the acceleration is easily computed by Equation [13]:

$$\vec{a}^n = \frac{\vec{f}^n}{m^n} \quad [13]$$

Once the acceleration is computed, the material velocity can be updated by Equation [14]:

$$\vec{v}^{n+1/2} = \vec{v}^{n-1/2} + \frac{\vec{a}^n}{2} \cdot (\Delta t^n + \Delta t^{n+1}) \quad [14]$$

Subsequently the Lagrangian node coordinate at t^{n+1} is computed by Equation [15]:

$$\vec{x}^{n+1} = \vec{x}_r^n + \vec{v}^{n+1/2} \cdot \Delta t^{n+1} \quad [15]$$

\vec{x}^{n+1} is the updated Lagrangian node coordinate at t^{n+1} and \vec{x}_r^n is the relaxed node coordinate after the advection phase at t^n . Note that, in a pure Lagrangian formulation there is no modification of the node coordinate during the mesh relaxation and $\vec{x}_r^n = \vec{x}^n$.

3.2. Mesh relaxation phase

For some problems, the element grid after the Lagrangian phase is rather distorted and a mesh relaxation phase is necessary to prevent a dropping time step size and, eventually, a negative Jacobian of some elements. Working with an Eulerian description of motion, the relaxation becomes trivial. It is a special case of the ALE formulation, where the mesh is moved back to its initial configuration. That is $\vec{x}_r^n = \vec{x}^0$. Relaxation algorithms used in most explicit codes, to handle more general situations, are linear combinations of the equipotential, simple average and volume average methods, as described in (Souli, 2000). The problem of the classical ALE formulation for shock and pressure wave problems is maintaining a fine mesh near the shock. Most of the methods for grid relaxation, the Winslow method developed in (Winslow, 1967), the Winslow-Crowley or the modified Winslow-Crowley grid relaxation algorithms developed in (Winslow, 1967) and implemented in hydrocodes, tend to control the grid spacing and produce a nearly uniform mesh in spherical and rectangular domains. There is a dominant reason for the lack of powerful mesh relaxation schemes suitable for the context of explicit time integration schemes. A good method should, if possible, not require the solving of large equation systems every time step. That would slow down each time integration cycle and eliminate the advantages of an explicit time integration scheme. The method proposed in this work does not involve any equation systems and it is easily implemented in existing Finite Element codes. The method is a simple function that operates on the configuration produced by an arbitrary relaxation scheme. To better capture the physics in the vicinity of shock fronts, the function delays the mesh relaxation.

$$\vec{x}_r^{n+1} = \vec{x}^{n+1} + \eta \left(\vec{x}_r^n - \vec{x}^{n+1} \right) \quad [16]$$

\vec{x}_r^n is a node coordinate provided by a mesh relaxation algorithm operating on the Lagrangian configuration at t^n and η is a relaxation delay parameter. A key issue is how to define η . The case $\eta = 0$ produces a pure Lagrangian formulation and $\eta = 1$ involves a pure Eulerian formulation. There are essentially two positive effects from forcing the mesh to partially follow the shock wave. Firstly, the mesh will contract in regions of large pressure gradients, which is beneficial for the accuracy in the Lagrangian phase of the simulation. Secondly, minimizing the advective fluxes in high gradient regions reduces dissipation and dispersion errors in the advection phase.

4. Numerical application

The performance of the proposed mesh relaxation scheme has been put to the test in a model of a mild steel plate subjected to an explosive blast loading, for which the experimental pressure loading was measured in (Boyd, 2000). The purpose is to compare the numerical pressure loads for different relaxation parameters η with the experimental pressure measured by a gauge at 100mm away from the center of the steel plate. This latter is a 1000mm square with a 5mm thick, which is clamped on the borders. The explosive is a sphere of Pentolite weighing 250 g, which is centrally detonated at 250mm away from the plate.

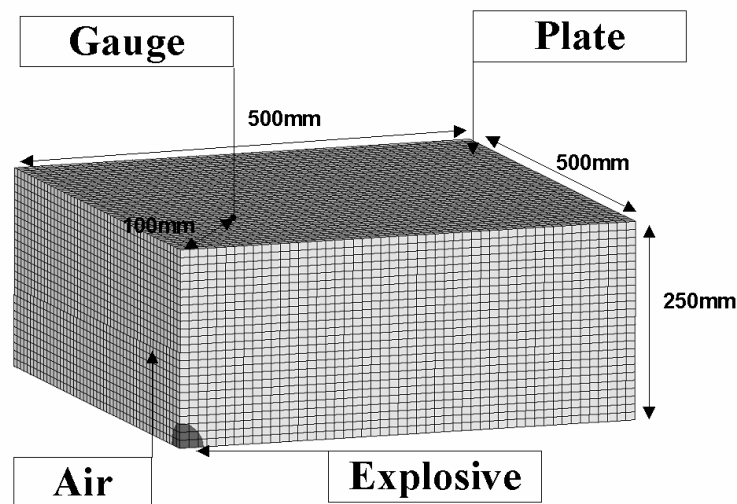


Figure 1. Mesh at $t = 0\mu s$

The mesh with three planes of symmetry is presented on Figure 1. The air mesh is a Cartesian ALE grid with a cubic mesh size of 1cm. The volume fraction of the explosive (Aquelet, 2005) is computed in the air mesh so that the explosive be a 1/8th of sphere with a radius of 32.9mm. The ignition point is applied at the center of the sphere. The high explosive material was modeled with the JWL (Jones-Wilkins-Lee) equation of state, which defines the pressure p^{he} with the Equation [17]:

$$p^{he} = A \left(1 - \frac{\omega}{R_1 V} \right) \exp(-R_1 V) + B \left(1 - \frac{\omega}{R_2 V} \right) \exp(-R_2 V) + \frac{\omega E^{he}}{V} \quad [17]$$

where A , B , R_1 , R_2 , ω are experimental constants. E is the specific internal energy in the material and $V = \rho_0^{he} / \rho^{he}$ is a ratio of the initial density and the current density of the material. The properties of the high explosive material modeled in this work are given in Table 1. In this table E_0^{he} is the initial specific internal energy, D is the detonation velocity and P_{cj} is the Chapman Jouget pressure.

Table 1. *Pentolite properties*

$A(\text{MBar})$	$B(\text{MBar})$	R_1	R_2	ω	$E_0^{he}(\text{MBar})$	$\rho_0^{he}(\text{g}\cdot\text{cm}^{-3})$
4.911	0.091061	4.4	1.1	0.3	0.08	1.67
$D(\text{cm}\cdot\mu\text{s}^{-1})$				$P_{cj}(\text{MBar})$		
0.747				0.25		

The air was modeled as an ideal gas and its pressure p^{air} can be expressed by Equation [18]:

$$p^{air} = (\gamma - 1) \frac{\rho^{air}}{\rho_0^{air}} E^{air} \quad [18]$$

with $\gamma = 1.4$. The air was initialized to a pressure of 1Bar by setting the initial internal energy to $E_0^{air} = 2.5\text{Bar}$ and the initial density to $\rho_0^{air} = 1.29 \times 10^{-3} \text{g.cm}^{-3}$.

The structure is composed of square shells with the same size. On Figure 1 the nodes at the interface of the air and structure meshes are tied in order to handle the fluid-structure interaction.

Figures 2 and 3 present a Lagrangian approach. The deformation pattern was too complex to be handled by a pure Lagrangian formulation and comparing simulations could not be performed as seen on Figure 3 where the mesh is highly distorted at $t = 50\mu\text{s}$. The Lagrangian calculation stops with a negative volume error. The obtained ALE results, shown in Figures 4 and 5, qualitatively display the mesh refinement in the vicinity of large pressure gradient regions at $t = 50\mu\text{s}$. The volume fraction of explosive gas shown in Figure 4 can be compared to Figure 3 for the Lagrangian approach. The mesh is more regular on Figure 4 than Figure 3. Figures 5, 6 and 7 show the pressure distribution at $t = 50\mu\text{s}$ before the reflection against the steel plate, $t = 100\mu\text{s}$ during the reflection, and $t = 150\mu\text{s}$ after the reflection. It is noticeable that the mesh is strongly refined in regions of large pressure gradients in the reflected wave.

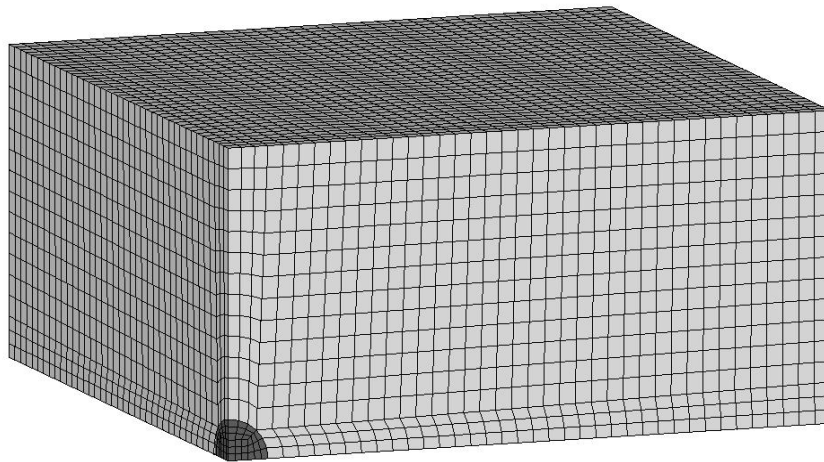


Figure 2. *Initial Lagrangian mesh*

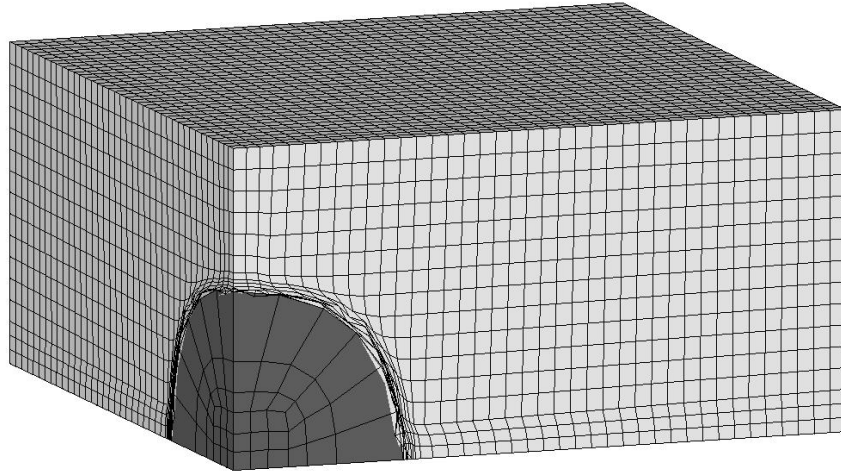


Figure 3. *Lagrangian mesh: volume fraction at $t = 50\mu s$*

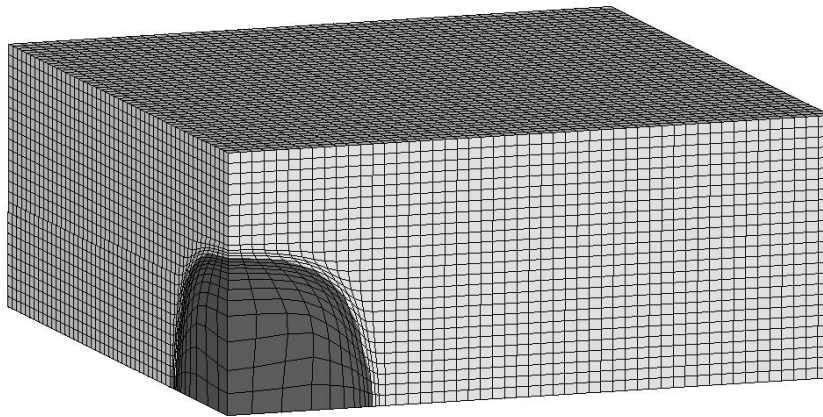


Figure 4. *ALE mesh: volume fractions at $t = 50\mu s$*

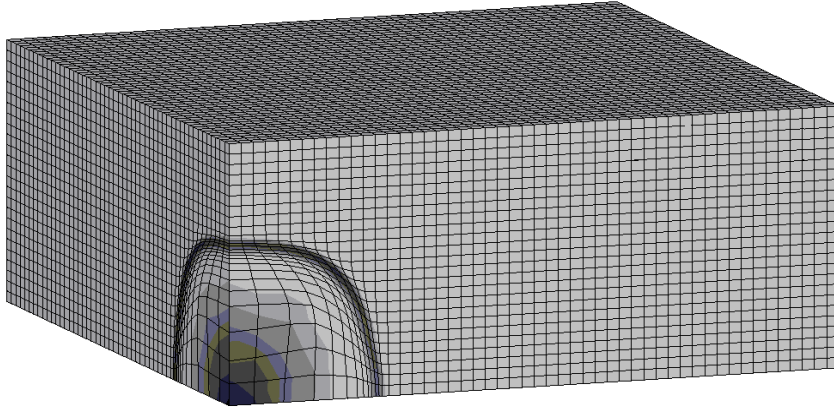


Figure 5. ALE mesh: shock wave at $t = 50\mu s$

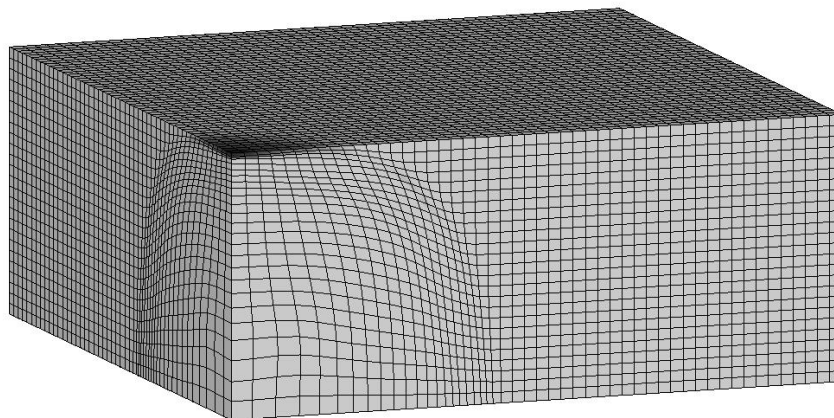


Figure 6. ALE mesh: shock wave at $t = 100\mu s$

A good relaxation scheme should manage to keep the mesh distortions on an acceptable level, while at the same time allow the mesh to follow the shock waves as well as possible. The issue is to adjust the relaxation parameter η . A small η can give an accurate result for the pressure. However if the mesh is too distorted in the vicinity of the shock, the computation will be jeopardized. A large η can preserve the regularity of the mesh but if the mesh is too coarse, the dissipative errors in the pressure will be too important. To give a range of acceptable values for η a parametric study is presented on Figure 7 and Table 2. The table presents the

numerical pressure peak at 100mm away from the center of the plate, the time of arrival of the peak and the computational elapsed time for different relaxation parameters, while Figure 8 compares the numerical pressure histories. The last row of Table 2 is the experimental pressure peak and time of arrival given by the report (Boyd, 2000). The calculations were run on a AMD Opteron® processor 252.

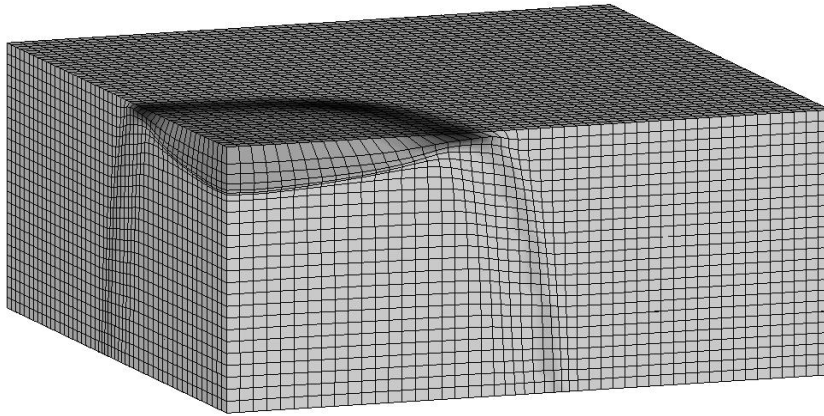


Figure 7. ALE mesh: shock wave at $t = 150\mu\text{s}$

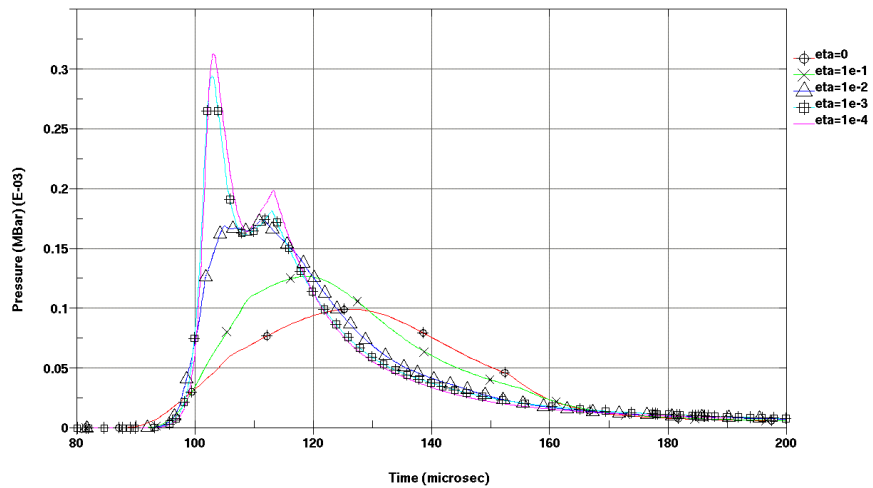


Figure 8. Numerical pressures for different relaxation parameters

Table 2. Numerical and experimental results

Relaxation parameter η	Pressure peak (MPa)	Time of Arrival (μs)	Elapsed time
1	9.9	126.5	4min-21sec
0.1	12.7	119	5min-6sec
0.01	16.9	105	13min-32sec
0.001	29.5	102.9	1h-16min-56sec
0.0001	31.3	103.2	11h-2min-39sec
Experimental data	40.0	100	-

Table 2 shows that the smaller the relaxation parameter η is, the closer to the experimental data the numerical results are. However the law is not linear because the results for $\eta = 0.001$ and $\eta = 0.0001$ are very close each other in respect with the other results. On Figure 8 the curves for $\eta = 0.001$ and $\eta = 0.0001$ are close, while the other pressure histories are disparate. The range of acceptable η for this problem should be between $\eta = 0.001$ and $\eta = 0.0001$. Nevertheless the computational elapsed time for $\eta = 0.0001$ is ten times longer than the one $\eta = 0.001$ and the run for $\eta = 0.0001$ terminates with a negative volume error. The suitable values of the relaxation parameter for this problem are around $\eta = 0.001$.

5. Conclusion

This paper has introduced a technique for delaying the mesh relaxation in ALE applications. The new method is an efficient tool for the treatment of shock waves. The function delaying the relaxation is simple and easily implemented in existing Finite Element codes. Delaying the mesh relaxation makes the description of motion more “Lagrange like”, contracting the mesh in the vicinity of the shock front. This is beneficial for the numerical accuracy, in that dissipation errors are reduced. Away from the shock, the method relaxes the mesh to eventually behave more as an Eulerian or a classical ALE equipotential method. The exact definition of the relaxation parameter is a issue for general applications of shock wave. However a good value of this parameter should be smaller than 0.01. The numerical application showed that the suitable relaxation parameter for the problem should be around 0.001.

6. References

- Aquelet N., Seddon C., Souli M., Moatamedi M., “Initialisation of volume fraction in fluid/structure interaction problem”, *IJCrash*, Vol. 10, No. 2, 2005.
- Belytschko T., Liu W.K., Moran B., *Nonlinear Finite Elements for Continua and Structures*, John Wiley & Sons, LTD, 2001.
- Belytschko T., Flanagan D. F., Kennedy J. M., “Finite element method with user-controlled meshes for fluid-structure interactions”, *Comput. Methods Appl. Mech. Engrg.*, Vol. 33, 1982, p. 682-723.
- Benson D.J., “Computational methods in Lagrangian and Eulerian Hydrocodes”, *Comput. Methods in Appl. Mech. Engrg.*, Vol. 72, 1992, p. 235-294.
- Boyd S.D., Acceleration of a Plate Subject to Explosive Blast Loading - Trial Results, Maritime Platforms Division Aeronautical and Maritime Research Laboratory, DSTO-TN-0270, 2000.
- Brooks A. N., Hughes T. J. R., “Streamline upwind/Petrov-Galerkin formulations for convection-dominated flows with particular emphasis on the incompressible Navier-Stokes equations”, *Comput. Methods in Appl. Mech. Engrg.*, Vol. 32, 1982, p. 199-259.
- Donea J., “Arbitrary Lagrangian-Eulerian finite element methods”, *Comput. Methods for Transient Analysis (A84-29160 12-64)*, 1983, p. 473-516.
- Hughes T. J. R., Liu W. K. and Zimmerman T. K., “Lagrangian-Eulerian finite element formulation for viscous flows”, *Comput. Methods Appl. Mech. Engrg.*, Vol. 21, 1981, p. 329-349.
- Hughes T. J. R., Mallet M., Mizukami A., “A new finite element formulation for computational fluid dynamics: II. Beyond SUPG”, *Comput. Methods Appl. Mech. Engrg.*, Vol. 54, 1986, p. 341-355.
- Liu W. K., Chang H., Chen J.-S. and Belytschko T., “Arbitrary Lagrangian-Eulerian Petrov-Galerkin finite elements for non-linear continua”, *Comput. Methods in Appl. Mech. Engrg.*, Vol. 68, 1988, p. 259-310.
- Mallet M., A finite element method for computational fluid dynamics, Ph. D. Thesis, Stanford University, Stanford, CA, 1985.
- Souli M., Ouahsine A., Lewin L., “ALE and Fluid-Structure Interaction problems”, *Comp. Meth. Appl. Mech. Engrg.*, Vol. 190, 2000, p. 659-675.
- Van Leer B., “Towards the Ultimate Conservative Difference Scheme, IV. A New Approach to Numerical Convection”, *Journal Computational Physics*, Vol. 167, 1977, p. 276-299.
- Wilkins M., “Calculation of elastic-plastic flow”, *Methods in Computational Physics*, Vol. 3, *Fundamental Methods in Hydrodynamics*, (Academics Press, New York, 1964), p. 211-263.
- Winslow A.M., “Numerical Solution of the Quasilinear Poisson Equation in a Nonuniform Triangle Mesh”, *J.Comput. Phys.*, Vol. 2, 1967, p. 149-172.
- Young D.L., “Time-dependent multi-material flow with large fluid distortion”, *Numerical Methods for Fluids Dynamics*, Ed. K. W. Morton and M.J. Baines, Academic Press, New-York, 1982.